JOURNAL OF CATALYSIS 56, 174–184 (1979)

X-Ray Photoelectron Spectroscopy/Secondary Ion Mass Spectrometry of FeRu Alloy Catalysts

G. L. OTT AND W. N. DELGASS

School of Chemical Engineering, Purdue University, West Lafayette, Indiana 47907

AND

N. WINOGRAD AND W. E. BAITINGER

Department of Chemistry, Purdue University, West Lafayette, Indiana 47907

Received July 6, 1978

XPS/SIMS investigation of unsupported FeRu alloys has shown that the reduced and passivated surface contains an iron phase in addition to the alloy phase. Carefully controlled SIMS studies produced smooth correlations of Ru^+ and Fe^+ yields with composition and indicate iron enrichment of the surface. Strong $FeRu^+$ ion yields, expected for intimately mixed surfaces, demonstrate the sensitivity of SIMS to local atomic structure. Chlorine impurities, present on the surface in significant amounts, were not removed by H_2 reduction at 823 K. The results suggest that chlorine impurities may affect chemisorption results and that the passivated surface of FeRu alloys is partially covered by thin islands of iron oxide.

INTRODUCTION

Nearly all solid catalysts contain more than one element. Most contain several phases. Quantitative analysis of the complex surface layer can indicate average composition and suggest surface structure. Perhaps most important for heterogeneous surfaces, however, is information on local composition, i.e., the proximity of the various elements on the surface to each other. With knowledge of local structure, we can begin to examine the origins of promotor action and the synergism in multicomponent catalysts.

A number of surface analysis techniques capable of probing catalysts have been developed in recent years. Each method has its strengths and limitations. Often the results sought come only when several of these tools are used in concert. In this research we are applying the combination X-ray photoelectron spectroscopy (XPS) and secondary ion mass spectrometry (SIMS). Both techniques have good sensitivity to impurities. XPS can identify chemical states and provide quantitative analysis of the average composition of the surface (*1–3*). SIMS, a new and still developing addition to the tools of the catalytic chemist, shows particular promise for revealing local surface structure (*4–6*). With this combination of capabilities, XPS/SIMS is well suited for probing multicomponent catalysts.

Two unique features of XPS make it particularly useful in catalytic studies. First, XPS examines only the first one to ten atomic layers of the sample. Photo-

0021-9517/79/020174-11$02.00/0

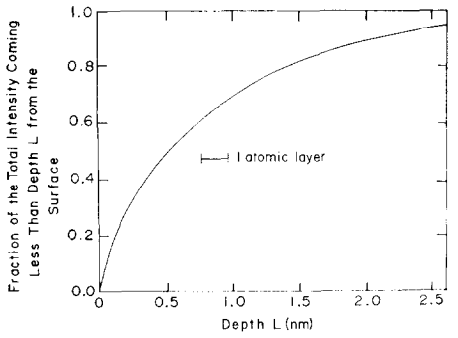

FIG. 1. Depth dependence of XPS intensity.

electrons which are ejected from surface atoms easily escape into the vacuum to be detected. Electrons ejected from subsurface layers, however, must travel through the material above before they can escape. The probability of escape without energy loss is given by $e^{-x/\lambda}$, where x is the distance to be traversed and λ is the mean-free path for inelastic collisions. Figure 1 shows the fraction of the XPS signal accounted for by atoms above depth L from the surface. The values of $\lambda = 1.5$ nm and layer thickness of 0.2 nm used in the calculation of Fig. 1 are typical.

The second useful feature of XPS is that the exact binding energy of the core electrons is sensitive to the number of valence electrons (i.e., the net charge) on the atom. Typical shifts are of order 1 eV per oxidation number while the peak width is 0.6–2 eV. Interpretation of chemical shifts is not without difficulties (*7*), but XPS can often provide direct observation of changes in surface chemical state of a catalyst. Measurement of sulfiding (*8*), oxidation/reduction (*9*), and adsorbate state (*10*) are a few of many successful studies to date.

Like XPS, SIMS uses a source of energy to induce emission of particles from the catalyst surface. Instead of X-rays, SIMS uses a beam of ions such as Ar^+ at energies from 200 to 20,000 eV. Instead of photoelectrons, atoms and clusters of several atoms are ejected from the surface. A fraction of the atoms or clusters leave as positive and negative ions which are detected with a mass spectrometer such as a quadrupole. Because of the emission of matter from the surface, the SIMS technique is inherently destructive. In the static mode (*4*), however, SIMS probes the initial surface since such low primary ion fluxes are used that the probability of examining a previously damaged portion of the surface is negligible. Understanding of the SIMS process is not yet complete, but recent advances in the calculation of the secondary emission of multiatom clusters show convincingly that clusters are formed over the surface from atoms which were close neighbors (*5*, *11*, *12*).

A SIMS spectrum is a plot of detected secondary ions/second versus mass to charge ratio, as shown in Fig. 2. The secondary ion current can be expressed as (*14*):

$$I_s = I_p \times A \times S \times \alpha^+ \times n_{spec} \times \theta_m.$$

I_s	Secondary ion current (ions detected/sec)
I_p	Primary ion current density (ions/(sec cm^2))
A	Sample area (cm^2)
S	Sputter yield (particles ejected per incident particle)
α^+	Ionization probability (particles ionized/ejected particle)
n_{spec}	Overall transmission function of spectrometer (ions detected/ion emitted)
θ_m	Fractional surface coverage of species producing the secondary ion.

The primary and secondary ion currents are measured in the spectrometer, while the transmission function can be estimated or canceled out in comparative work. Sputter yields for some elements have been measured gravimetrically (*15*). The effective ionization probability is not well understood but depends on such properties as the ionization potential of the atom

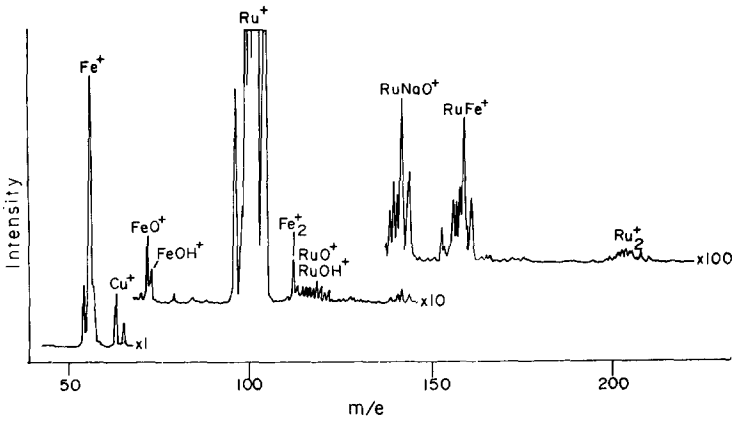

FIG. 2. SIMS spectrum of reduced and passivated 15Fe85Ru powder at a primary ion flux of 7×10^{-9} A/cm² (*13*).

(or multiatom cluster) and the electronic properties of the surface. In short, sensitivity factors needed for quantitative analysis from secondary ion yields are not yet readily available. Nevertheless, SIMS can make important contributions to catalyst studies with its sensitivity to surface hydrogen, its sampling depth of one to two atomic layers, and its ability, through the multiatom cluster ions, to probe the local atomic environment on the surface.

In this work we are attempting to exploit the multimetallic cluster concept (*16*) to develop new, more selective catalysts for hydrocarbon synthesis from CO and H_2 and have started with the FeRu system. For FeRu supported on SiO_2, Vannice *et al.* (*17*) report a maximum in olefin to paraffin ratio and in the selectivity to higher hydrocarbons at Fe/Ru atom ratios between 0.5 and 2. High yields of propylene with Fe/Ru on SiO_2 have also been noted in this laboratory (*18*). Confirmation of the intimate mixing of Fe and Ru by Mössbauer spectroscopy (*17*, *19*) supports association of these kinetic effects with bimetallic cluster formation.

This paper presents an analysis of unsupported FeRu alloy powders. The powders have high enough surface area to permit catalytic measurements, and as will be shown, present a complex surface structure. Development of analytical techniques for understanding these surfaces will provide a basis for interpreting the additional perturbations caused by the presence of a catalyst support.

EXPERIMENTAL

Materials

The Fe/Ru powders were prepared from $RuCl_3 \cdot H_2O$ (Englehard) and $Fe(NO_3)_3$ (Mallinckrodt) solutions by hydrazine reduction (*20*) and given to us by R. L. Garten. In the preparation procedure appropriate amounts of the metal salts were dissolved in 200 ml of deionized water. The salt solution was then slowly added to a reducing solution of NH_4OH and N_2H_4 in 200 ml of deionized, oxygen-free water under vigorous agitation. The resulting slurry was filtered and the filter cake washed with water and air dried at 110°C to yield a fresh catalyst.

Fresh catalysts were then pressed into 7-mm-diameter pellets, 1–2 mm thick, and reduced in 8% H_2 in He at 300°C overnight. The reduced catalysts were passivated by exposure to 0.1 to 0.5 Torr of ultra-high purity O_2 (Matheson) before their short exposure to air during loading into the spectrometer. Pure Ru powder was prepared in the same fashion as the alloys.

Reduced samples had surface areas of 7–15 m^2/g. In the designations mFenRu m and n are atom percentages.

XPS/SIMS

A Hewlett Packard Model 5950A X-ray photoelectron spectrometer using Al$K\alpha$ X rays (1487 eV) produced the XPS spectra of the passivated sample pellets held in a gold-plated mount. Assignment of the value of 84.0 eV for the Au($4f_{7/2}$) line of an Ar^+ etched Au foil established the binding energy calibration (*21*). The custom-built SIMS equipment used in this work utilizes a Riber Model Q156 quadrupole mass analyzer housed in a Perkin Elmer TNB-X belljar. A Danfysik 911 ion delivery system is interfaced to the UHV belljar via three stages of differential pumping. The system, described in more detail elsewhere (*22*, *23*), features high resolution and sensitivity up to mass 800, a wide choice of mass-selected primary ion beams, and ultra-high vacuum transfer of samples between SIMS and XPS. Sample pretreatment and mounting for SIMS is identical to that for XPS.

RESULTS AND DISCUSSION

Unsupported FeRu alloys are good samples for spectroscopy because they give strong signals (minimizing counting times), they do not experience charge buildup during photon or ion bombardment, and they avoid the need to consider effects of support structure. In the sections to follow, we present combined XPS/SIMS results on surface phases and structure, composition, and purity and discuss the catalytic implications of these findings.

Surface Phases and Structure

Here we compare the chemical state of the fresh catalyst to that of the reduced and passivated one and then discuss the structure and chemistry of the passivated surface in detail. Figure 3 shows the Fe($2p_{3/2-1/2}$) and Ru($3d_{5/2-3/2}$) regions of the XPS spectra for the fresh and reduced/passivated 76Fe24Ru catalyst. The fresh catalyst, which was air dried at 110°C, showed a Ru($3d_{5/2}$) peak at 282.8 eV and Fe($2p_{3/2}$) peaks at 710 and 712 eV. After reduction and passivation with O_2, the Ru($3d_{5/2}$) peak shifted to 280.1 eV. The Fe($2p_{3/2}$) peaks at 710 and 712 eV re-

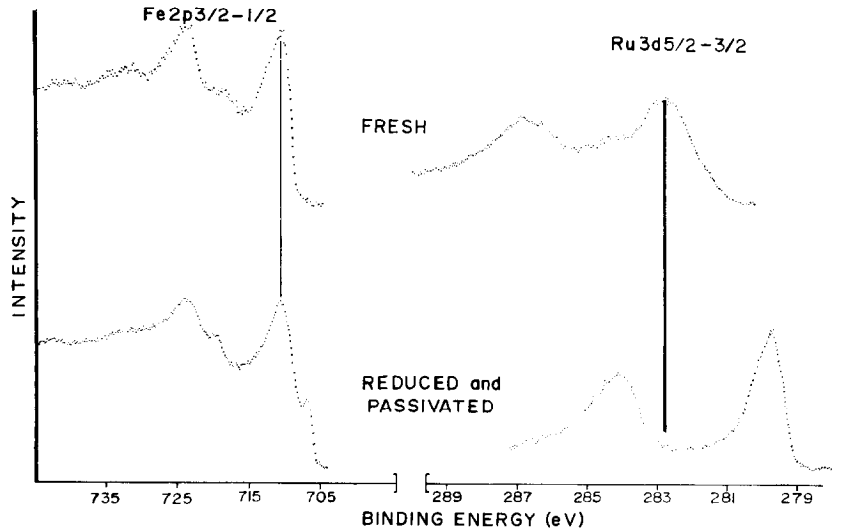

FIG. 3. XPS spectra of fresh and reduced/passivated 76Fe24Ru powder.

TABLE 1

Binding Energies for Ru($3d_{5/2}$) (*21*) and Fe ($2p_{3/2}$) (*24*)[a]

Species	E_b
Ru (Ru^0)	280.0
RuO_2 (Ru^{4+})	280.7
RuO_3 (Ru^{6+})	282.5
RuO_4 (Ru^{8+})	283.3
Fe (Fe^0)	708.2
$K_4Fe(CN)_6$ (Fe^{2+})	710.2
$K_3Fe(CN)_6$ (Fe^{3+})	711.6
Fe_2O_3 (Fe^{3+})	712.4
Fe_2O_3 (Fe^{3+})	712.4

[a] Ru referenced to Au($4f_{7/2}$) as 84.0 eV; Fe referenced to C(1*s*) impurity at 285.0 eV.

mained and a new peak appeared at 707 eV. The higher binding energy peaks in the Fe and Ru regions correspond to Fe($2p_{1/2}$) and Ru($3d_{3/2}$) electrons. XPS studies of the oxidation of Ru by Kim and Winograd (*21*) and Fe by Kishi *et al.* (*24*) are summarized in Table 1. On the basis of these assignments we conclude that the fresh catalyst is a mixed oxide of Fe and Ru with Fe^{2+}, Fe^{3+}, and Ru^{6+} present. After reduction and passivation, all of the Ru appears to be metallic (Ru^0) and some of the Fe exists as Fe^0 in addition to Fe^{2+} and Fe^{3+}. Note that the presence of Ru^0 only does not preclude adsorption of oxygen on the exposed Ru surface. It is characteristic of many metal surfaces that adsorbed O_2 appears clearly in the O(1*s*) spectrum but does not perturb the metal core electron energies significantly until place exchange occurs and oxygen begins to enter the metal lattice (*25–27*). Since the data for FeRu alloys show oxidized Fe but no oxidized Ru we conclude that a phase separation occurs, producing an iron oxide phase containing little or no Ru. The degree of alloying of the remaining Fe^0 and Ru^0 cannot be determined from these measurements, so we turn to SIMS for further structural information.

Figure 2 gives the SIMS data for reduced and passivated 15Fe85Ru. Figure 4 gives the expected line spectra of several important ions calculated from tables of natural isotopic distributions of the elements and confirms the assignments made in Fig. 2. The presence of Ru-containing ions in Fig. 2 indicates that the catalyst is not completely covered by a skin of iron oxide. In that case no Ru would be accessible to the SIMS measurement. The presence of FeO^+ and $FeOH^+$ are indicative of oxidized iron and illustrate the sensitivity of the technique to hydrogen, present in this case because of interaction of the sample with H_2O in the air or spectrometer background. The RuO^+ and $RuOH^+$ ions indicate the presence of chemisorbed oxygen and water as expected but, as discussed earlier, not visible in XPS of Ru lines. The $RuNaO^+$ ion ($m/e \simeq 141$) is noteworthy because Na, an ubiquitous low-level impurity, is present

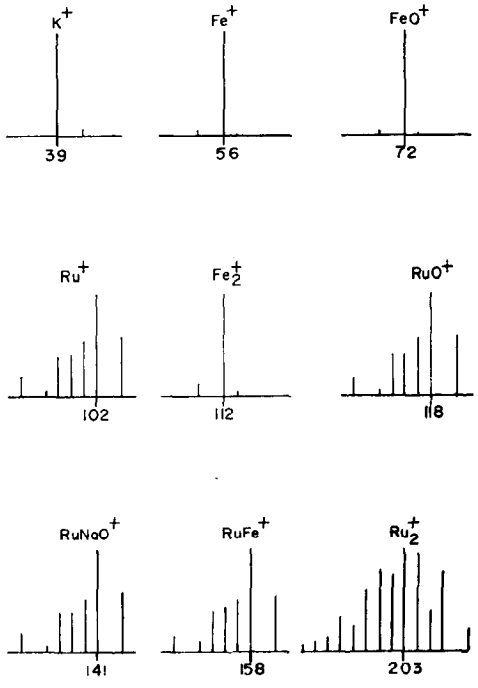

FIG. 4. Relative isotopic yields for various ions based on natural isotopic abundance of the elements (*13*).

on the surface in less than 0.1% of a monolayer quantities (i.e., it is not visible in the XPS spectrum). Detection of $RuNaO^+$ and large peaks (not shown) for Na^+ and NaO^+ reflect the high sensitivity of SIMS to alkali metals due to high ionization probabilities. The Cu^+ ions in the spectrum come from the sample holder.

The most interesting feature of Fig. 2 is the presence of metal dimer ions. The $FeRu^+$ ion indicates close proximity of iron and ruthenium in the sample and is taken as indicative of alloy formation. A physical mixture of pure Fe and pure Ru powders showed enhanced Fe_2^+ and Ru_2^+ emission with virtually no $RuFe^+$ emission, as expected.

Together, the XPS/SIMS data discussed so far identify an iron oxide phase, an iron/ruthenium alloy phase, and chemisorbed oxygen in the surface region. Atomic absorption analysis for Fe and Ru showed by difference that negligible oxygen was incorporated into the bulk. The depth of the iron oxide phase on the surface was probed by comparing spectra of iron XPS lines with different kinetic energy. Since the mean free path for inelastic scattering increases with electron kinetic energy, peaks for more weakly bound core levels correspond to higher electron kinetic energy and, therefore, reflect the chemistry at a greater average depth from the surface. In Fig. 5, for 67Fe33Ru, the Fe(3*p*) electrons, with ca. twice the kinetic energy of the Fe($2p_{3/2}$) electrons, show a larger fraction of the total intensity as Fe^0. Curve resolution was done on a Dupont Model 310 curve resolver. Linewidths assigned to Fe^0 are in reasonable agreement with experimental values for reduced FeRu alloys. Thus, we conclude that although the oxidized iron is in a three-dimensional oxide phase, that phase is restricted to a surface region of the order of 1.0 nm thick. To test this interpretation we argon-ion bombarded the surface for 1 hr with an ion current density of 2×10^{-7} A/cm^2; sputtering off about three atomic layers of material. The increase in the amount of Fe^0 in the XPS spectrum of the surface after bombardment, Fig. 6, is consistent with the idea that the outermost layers of the surface contain more Fe oxide. We note, however, that Fe^0 can be enhanced either by iron oxide removal or Ar^+ induced reduction (*28*). Increased visibility and decreased chemisorbed oxygen coverage of the alloy phase after sputtering produce a threefold increase in the $FeRu^+/Ru^+$ yield ratio in the SIMS spectrum. The picture of the surface emerging from all these results is one in which an FeRu alloy phase with varying composition is partially covered by thin patches of iron oxide and the entire surface is covered by chemisorbed oxygen and water.

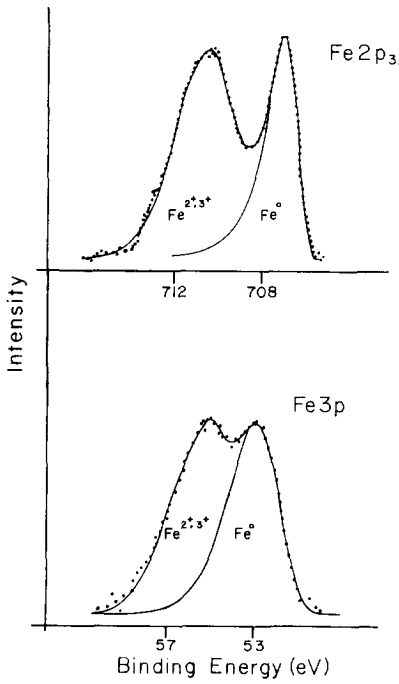

FIG. 5. XPS spectra for reduced and passivated 67Fe33Ru.

Surface Composition

The previous section illustrates that even an unsupported alloy surface can

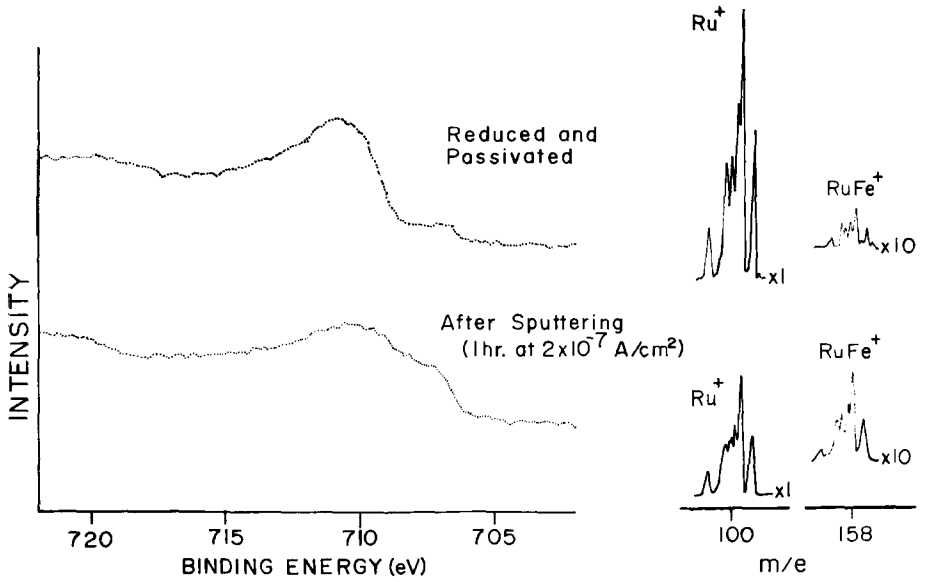

FIG. 6. XPS and SIMS spectra of 48Fe52Ru powder before and after sputtering.

exhibit significant compositional heterogeneity. Thus, one must beware of quantitative results averaged over the entire surface and place a premium on analysis of local composition of the first monolayer. With this caution in mind, we examine the quantitative features of XPS/SIMS data on FeRu powders.

Quantitative SIMS is complicated by large changes in ion yield as a function of the degree of oxidation of the surface. In order to minimize this difficulty, we adopted a strict pretreatment procedure in which each sample was reduced in H_2 at 300°C, cooled to room temperature in flowing ultrahigh purity argon, evacuated for 10 min at 10^{-4} Torr, and then passivated by exposure to 0.1 to 0.5 Torr of ultrahigh purity oxygen for 15 min. After passivation, samples were stored at 10^{-4} Torr for transfer to the SIMS apparatus. They were loaded into the spectrometer with 1- to 3-min exposure to air.

In addition to standardizing the pretreatment procedure, we verified the constancy of the spectrometer performance by reference to a pure Ru powder standard. Passivated Ru powder was not oxidized in depth and gave constant secondary ion yields even after air exposure of several hours. The quantitative SIMS measurements were obtained by mounting an alloy and an Ru standard on opposite faces of the sample holder so that comparison of the two required only a 180° rotation of the precision manipulator while all other factors were held constant. Care was also taken to minimize surface damage by working well into the static SIMS mode. With the primary beam flux of (1–3) $\times$ 10^{-10} A/cm^2 and a sputter yield of one, a 30-min experiment removed less than 0.2% of an atomic layer.

The data in Fig. 7 show that the careful experimental procedure leads to reproducible and self-consistent results. The invariance of the Ru^+ yield from the standard confirms the constancy of the spectrometer performance, while Fe^+ and Ru^+ ion yields from the alloys show a smooth variation in accord with changes in bulk composition. The striking features of the plot are the linearity of the ion yield variations, the low values of the Ru^+ yield from the alloy compared to the standard, and the fact that linear extrap-

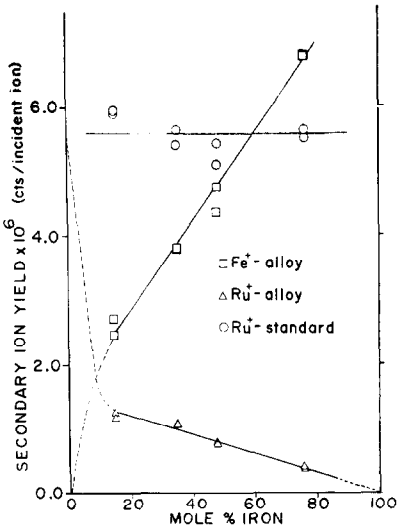

FIG. 7. SIMS yields for an Ru standard and FeRu alloys with varying composition.

olation of the Fe^+ line does not pass through the origin. These qualitative features are consistent with the proposed model of the surface structure. Both the low Ru^+ yields and the nonzero intercept of the iron line can be accounted for by the presence of iron oxide islands. The overlayer shields much of the Ru from view and thus lowers the Ru^+ yield. The presence of the islands also contributes an Fe^+ yield that does not necessarily change directly with average sample composition and thus does not extrapolate to zero at low iron content. The quantitative merit of the model and the linearity of the plot cannot be evaluated without more complete knowledge of the SIMS process. We find the consistency of the data encouraging, however, and anticipate increasingly accurate surface phase analysis from SIMS as the technique continues to develop.

While SIMS carries information primarily concerning the surface layer itself, XPS includes the depth contribution already discussed. Attempts to analyze composition as a function of depth were frustrated in this particular case because the steep background in the Fe(2*p*) region of the spectrum (see Fig. 3) made accurate determinations of the relative peak areas in that region difficult. The Fe(3*s*) and Ru(4*s*) peaks were easier to fit. Since they correspond to nearly identical electron kinetic energies, peak areas of these lines provide quantitative data averaged over the same depth. Results for the two higher Fe-content catalysts are compared to the bulk composition ratio in Table 2. The intensity (peak areas) divided by the cross section for photoemission, σ, is proportional to elemental concentration. Thus Table 2 indicates an iron enrichment of the surface layer. This result is consistent with the structural model of the surface because the iron oxide islands are presumed to contain no Ru and their presence would cause an increase in the Fe/Ru ratio as long as the FeRu alloy phase at the surface is not significantly enriched in Ru. We conclude, therefore, that the Ru-rich phase which must accompany the Fe-rich one is not at the surface but beneath the iron oxide islands.

Surface Purity

Intentional alteration of the surface purity of catalysts by addition of promotors or inhibitors is a well-known method of controlling catalytic behavior (*29*). Clearly, unintentional introduction of impurities from a gas stream or catalyst preparation procedure can also influence catalyst function. For the FeRu powders considered here the important impurity is chlorine, presumably from the $RuCl_3$ used in the preparation. Examination of the 0–1000 eV XPS scan of the 15Fe85Ru powder, Fig. 8, shows a surprisingly large

TABLE 2

Quantitative XPS

(x_{Fe}/x_{Ru}) bulk	$[(I/\sigma)_{Fe(3s)}/(I/\sigma)_{Ru(4s)}]$
0.92	1.47
3.17	3.29

Cl(2*p*) peak in addition to the expected peaks for Fe, Ru, and O. Since XPS is three times as sensitive to Ru($3d_{5/2}$) as to Cl(2*p*), the level of chlorine in the surface region is significant.

SIMS detects the chlorine impurity as $FeCl^+$ and Cl^- as shown in Fig. 9. $RuCl^+$ was not present. Since the $FeCl^+$ yield was largest for the 24Ru76Fe sample and XPS showed a factor of 2–3 less chlorine on pure Ru powder samples compared to the alloys, the data suggest that the retention of chlorine on the metal surface is enhanced in the presence of iron. Whatever its bonding, the chlorine impurity on FeRu powders is remarkably stable. Attempts to remove chlorine from 15Fe85Ru powder are recorded in Table 3. Removal by H_2 was small compared to that by exposure of the alloy surface to a 3/1 mixture of H_2/CO synthesis gas at 538 K. Presumably, in the latter case, the Cl leaves as a chlorinated hydrocarbon, as found by Vannice for supported transition metal catalysts (*30*). It is interesting to note that in the present case the Cl resides on the metal and not, as is often presumed for supported catalysts, on a support. Since the chlorine level is reduced by reaction of CO and H_2 it may not have a major effect on catalytic activity. Further work using SIMS to monitor chlorine levels before and after reaction is being done.

Since the chlorine is not removed by typical pretreatments in H_2, it may well have a significant effect on the adsorption behavior of Ru and FeRu alloys. It could, in fact, contribute to the result found by Garten (*20*) and confirmed in our laboratory that there is a large fraction of the surface of these materials which is inaccessible to H_2 chemisorption. By measuring the total surface area of a powder with the BET method (*31*), one can determine the total number of atoms exposed assuming a value of 7.6 Å²/metal atom. H_2 chemisorption done at room temperature showed uptakes corresponding to only 20 to 30% of the surface being covered with hydrogen (assuming that one H atom bonds to one metal

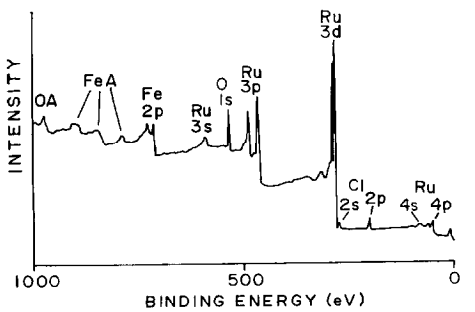

FIG. 8. Broad scan XPS spectrum for reduced and passivated 15Fe85Ru powder.

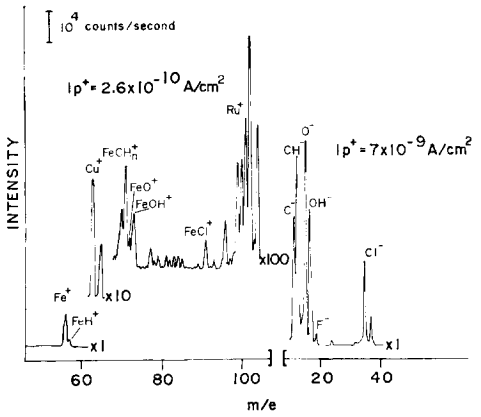

FIG. 9. Positive and negative ion SIMS spectra for 35Fe65Ru powder.

TABLE 3

Chlorine Removal from 15Fe85Ru Catalyst Powder

Treatment[a]	$[(I/\sigma)_{Cl(2p)}/(I/\sigma)_{Ru(3d5/2)}]$
573 K; H_2 100 cc/min 2 hr	0.375
823 K; H_2, 100 cc/min 8 hr	0.272
538 K; $CO/3H_2$, 100 cc/min 2 hr followed by	
573 K; H_2, 100 cc/min 8 hr	0.056

[a] All treatments at 1 atm.

surface atom). It is apparent that caution is warranted in interpretation of catalytic data from surfaces of questionable purity.

CONCLUSIONS

XPS and SIMS have been used to probe the surface structure, composition, and purity of a series of unsupported FeRu powder catalysts. Analysis of the depth dependence and chemical state information in the XPS/SIMS data suggests that the reduced and passivated surface of the FeRu powder is an FeRu phase partially covered by islands of pure iron oxide. Chemisorbed oxygen and water cover both phases as well. Structure interpretation is based on XPS data which show Fe^0, Fe^{2+}, Fe^{3+}, and Ru^0 but no ruthenium oxides and also indicate, through the depth dependence of the lines from different Fe core levels, that the oxidized iron is concentrated near the surface. The presence of Ru in the uppermost layer is indicated by Ru-containing ions in the SIMS spectrum. Semiquantitative treatment of the data shows iron enrichment of the surface and is consistent with the proposed model. Systematic variations of the SIMS data with bulk composition shows that careful sample pretreatment can lead to consistent results in spite of the high sensitivity of SIMS yields to small changes in surface state.

Perhaps the most significant result is the observation by both XPS and SIMS of a surprisingly high level of chlorine impurity on the powder surface. The chlorine level was greatly reduced during the CO + H_2 synthesis reaction at 538 K but remained even after pretreatment in H_2 at 823 K. The presence of surface chlorine after pretreatments typical for adsorption experiments suggests that this impurity may contribute to the discrepancy found between hydrogen uptakes and total (BET) surface areas (*20*).

ACKNOWLEDGMENTS

It is a pleasure to acknowledge R. L. Garten, Exxon Research and Engineering Company, for contributing the samples; R. L. Garten and M. A. Vannice for preprints and informative discussions; and the National Science Foundation for Grants MPS-7509308 and DMR76-00889A1 supporting this work.

REFERENCES

1. Siegbahn, K., Nordling, C., Fahlman, A., Nordberg, R., Hamrin, K., Hedman, J., Johansson, G., Bergniark, T., Karlsson, S.-E., Lindgren, I., and Lindberg, B., ESCA—Atomic, molecular and solid state structure by means of electron spectroscopy, *Nova Acta Regiae Soc. Sci. Upsal. (IV)*, **20**, Almquist and Wicksells, Uppsala (1967).
2. Delgass, W. N., Hughes, T. R., and Fadley, C. S., *Catal. Rev.* **4**, 179 (1970).
3. Delgass, W. N., Haller, G. L., Kellerman, R., and Lunsford, J. H., "Spectroscopy in Heterogeneous Catalysis," Academic Press, New York, 1979.
4. Benninghoven, A., *Surf. Sci.* **53**, 596 (1975).
5. Winograd, N., Harrison, D. E., Jr., and Garrison, B. J., *Surf. Sci.*, **78**, (1978).
6. Fleisch, T., Winograd, N., and Delgass, W. N., *Surf. Sci.*, **78**, 141 (1978).
7. Shirley, D. A., *Adv. Chem. Phys.* **23**, 85 (1973).
8. Patterson, T. A., Carver, J. C., Leyden, D. E., and Hercules, D. M., *J. Phys. Chem.* **80**, 1700 (1976).
9. Brinen, J. S., Schmidt, J. L., Doughman, W. R., Achorn, P. J., Siegel, L. A., and Delgass, W. N., *J. Catal.* **40**, 295 (1975).
10. Yates, J. T., Jr., Madey, T. E., and Erickson, N. E., *Surf. Sci.* **43**, 257 (1974).
11. Harrison, D. E., Jr., Kelly, P. W., Garrison, B. J., and Winograd, N., *Surf. Sci.* **76**, 311 (1978).
12. Garrison, B. J., Winograd, N., and Harrison, D. E., Jr., *J. Chem. Phys.* **69**, 1440 (1978).
13. Shepard, A., Hewitt, R. W., Baitinger, W. E., Slusser, G. J., Winograd, N., Ott, G. L., and Delgass, W. N., in "Quantitative Surface Analysis of Materials," (N. S. McIntyre Ed.), page 187, ASTM STP 643, (1978).
14. Dawson, P. T., and Walker, P. C., *in* "Experimental Methods in Catalytic Research" (R. B. Anderson and P. T. Dawson, Eds.), Vol. III, p. 250, Academic Press, New York, 1976.
15. Oechsner, H., *Appl. Phys.* **8**, 185 (1975).
16. Sinfelt, J. H., *J. Cat.* **29**, 308 (1973).
17. Vannice, M. A., Lam, Y. L., and Garten, R. L., Div. of Petroleum Chemistry pre-

print, Vol. 23, p. 495, ASC National Meeting, Los Angeles, Calif., March 1978.

18. Lauderback, L., M.S. Thesis, Purdue University, 1977.

19. Fortunato, F. A., Aschenbeck, D. P., and Delgass, W. N., to be published.

20. Garten, R. L., private communication.

21. Kim, K. S., and Winograd, N., *J. Catal.* **35**, 66 (1974).

22. Hewitt, R. W., Shepard, A. T., Baitinger, W. E., Winograd, N., and Delgass, W. N., *Rev. Sci. Instrum.*, submitted.

23. Fleisch, T., Shepard, A. T., Ridley, T. Y., Vaughn, W. E., Ott, G. L., and Delgass, W. N., *J. Vac. Sci. Tech.*, **15**, 1756 (1978).

24. Kishi, I., Oheda, K., and Ikeda, S., *Bull. Chem. Soc. Japan* **46**, 341 (1973).

25. Brundle, C. R., *Surf. Sci.* **48**, 99 (1975).

26. Krishnan, N. G., Delgass, W. N., and Robertson, W. D., *Surf. Sci.* **57**, 1 (1976).

27. Fuggle, J. C., and Menzel, D., *Chem. Phys. Lett.* **33**, 37 (1975).

28. Kim, K. S., and Winograd, N., *Surf. Sci.* **43**, 625 (1974).

29. Dry, M. E., Shingles, T., Boshoff, L. J., and Oosthuizen, G. J., *J. Catal.* **15**, 190 (1969).

30. Vannice, M. A., *J. Catal.* **37**, 449 (1975).

31. Brunauer, S., Emmett, P. H., and Teller, E., *J. Amer. Chem. Soc.* **60**, 309 (1938).